Effect of Cholera Toxin and Cyclic Adenosine Monophosphate on Fluid-Phase Endocytosis, Distribution, and Trafficking of Endosomes in Rat Liver

REBECCA W. VAN DYKE*

In prior studies, we showed that cholera (CTX) and pertussis toxins (PTX) increase rat liver endosome acidification. This study was performed to characterize the effects of these toxins and cyclic adenosine monophosphate (cAMP) on endosome ion transport, fluid-phase endocytosis (FPE), and endosome trafficking in liver. In control liver, more mature populations of endosomes acidified progressively more slowly, but both toxins and cAMP caused retention of an early endosome acidification profile in maturing endosomes. CTX caused a density shift in endosomes, and all agents increased net FPE at time points from 5 to 60 minutes. By confocal microscopy, fluorescent dextrans first appeared in small vesicles at the hepatocyte sinusoidal membrane and trafficked rapidly to the pericanalicular area, near lysosomes and the trans-Golgi network (TGN). Prolonged exposure to these agents caused redistribution of many labeled vesicles to the perinuclear region, colocalized with markers of both early (EEA1 and transferrin receptor) and late (LAMP1) endosomes. We conclude that cAMP is the common agent that disrupted normal maturation and trafficking of endosomes and increased net FPE, in part via decreased diacytosis. (HEPATOLOGY 2000;32:1357-1369.)

Endocytosis and vesicular transport are important functions of all cells, but they are particularly critical to liver, a polarized epithelia that has direct contact with blood, secretes a wide variety of essential plasma proteins, removes many macromolecules from blood, and transfers them to bile.[1] Endosomes are not static structures, because, during vesicular transport, endosomes remodel and their contents and membrane receptors are sorted and segregated into multiple types of vesicles with different destinations.[2,3] Endocytic vesicles also contain a specific complement of membrane ion transporters, some of which acidify the endosome interior space (the electrogenic V-type H^+–adenosine triphosphatase [ATPase]) or regulate the degree of acidification.[4,5] Although function of these transporters might be altered directly by classic signal transduction pathways, during normal endosome remodeling/maturation, vesicle ion transporters also may be sorted and redistributed, potentially leading to changes in the acidification parameters of late compared with early endosomes. For example, we previously showed that Na^+/H^+ exchange, which alters endosome interior pH (pH_i), is only detected in early (2-minute) endosomes.[5] Because pH_i itself may affect endosome function/trafficking,[6,7] sorting of vesicle ion transporters might, in turn, alter vesicle function.

Furthermore, the rates and/or mechanisms of endocytosis, exocytosis, and transcytosis are not necessarily constant. Cyclic adenosine monophosphate (cAMP) and/or heterotrimeric G proteins have been proposed to regulate a variety of steps in vesicle transport.[8-10] For example, some membrane transporters are regulated through cAMP-mediated changes in removal by endocytic vesicles or insertion from exocytic vesicles, which in turn may alter fluid-phase endocytosis (FPE).[11] In liver, the basolateral sodium-coupled taurocholate transporting protein (Ntcp) and some canalicular transporters are so regulated.[12,13] In our own previous work, cholera (CTX) and pertussis (PTX) toxins increased both liver cAMP and the rates and extent of acidification of liver endocytic vesicles loaded with a fluorescent probe of FPE, fluorescein isothiocyanate (FITC)-dextran.[14] Furthermore, these agents caused retention in older endosomes of active Na^+/H^+ exchange. Differences in endosome acidification might be the result of changes in the turnover rate or number of active proton pumps, or in the surface-to-volume ratio of endosomes.[15-17] However, these changes in endosome ion transporters might also reflect more global changes in the remodeling/maturation of early to late endosomes.

We, therefore, undertook these studies to develop methods to systematically assess parameters of endocytosis and vesicle trafficking in rat liver. These methods were used to determine the effects of short-term (dibutyryl cAMP) and long-term (CTX, PTX, and dibutyryl cAMP) increases in cAMP on liver FPE, and to provide evidence for the hypothesis that cAMP impairs remodeling/maturation of liver FPE endosomes derived from the sinusoidal membrane. We chose to use *in vivo* liver for these studies because of its physiologic relevance and

Abbreviations: ATPase, adenosine triphosphatase; pH_i, intravesicular pH; cAMP, cyclic adenosine monophosphate; FPE, fluid-phase endocytosis; Ntcp, sodium-coupled taurocholate transporting protein; CTX, cholera toxin; PTX, pertussis toxin; FITC, fluorescein isothiocyanate; TR, Texas red; WGA, wheat germ agglutinin; LAMP-1, lysosome-associated membrane protein; MRP-2, multidrug resistance–related protein 2; EEA1, early endosomal antigen 1; TGN, trans-Golgi network; PNS, postnuclear supernatant; APDE-I, alkaline phosphodiesterase I; PBS, phosphate-buffered saline; TBST, Tris-buffered saline with Tween; MVB, multivesicular bodies.

From the Department of Medicine, University of Michigan Medical School and Veterans' Administration Hospital, Ann Arbor, MI.

Received June 8, 2000; accepted September 5, 2000.

*Technical assistance was provided by Marianne R. Lewis, Xiaqing Wang, and Douglas W. Barns.

Funded by grants from the Veterans Administration (Merit Review) and the NIH (R01 DK-38333).

Address reprint requests to: Rebecca W. Van Dyke, 6520 MSRB-I, University of Michigan Medical School, 1150 W. Medical Center Dr., Ann Arbor, MI 48109-0682. E-mail: wynne@umich.edu; fax: 734-763-2535.

0270-9139/00/3206-0022$3.00/0
doi:10.1053/jhep.2000.19790

because both liver perfusion[18] and hepatocyte isolation[19] themselves appear to affect endocytosis.

MATERIALS AND METHODS

Materials. Seventy thousand– and 10,000-d FITC-dextrans and other chemicals were from Sigma Chemicals (St. Louis, MO); 10,000-d and 70,000-d Texas red–dextrans (TR-dextran), FITC–wheat germ agglutinin (WGA), and anti-fluorescein antibody were from Molecular Probes, Inc. (Eugene, OR); CTX and PTX were from List Biological Laboratories, Inc. (Campbell, CA); Percoll and density marker beads were from Pharmacia Biotech (Piscataway, NJ); VectaShield was from Vector Laboratories, Inc. (Burlingame, CA); and sodium dodecyl sulfate–polyacrylamide gel electrophoresis (SDS/PAGE) and Western blot supplies were from Bio-Rad Laboratories (Hercules, CA), Amersham Life Science (Little Chalfont, England), and Pierce (Rockford, IL).

Antibodies. Polyclonal antibodies to rab 5, rab 7, and lysosome-associated membrane protein 1 (LAMP-1) were from Santa Cruz Biotechnology, Inc. (Santa Cruz, CA). Polyclonal antibody against multidrug resistance-related protein 2 (MRP-2) was the gift of Dr. Dietrich Keppler (University of Heidelberg). Mouse monoclonal antibodies were purchased to transferrin receptor (Zymed Laboratories, South San Francisco, CA), early endosome antigen 1 (EEA1) (Transduction Laboratories, Lexington, KY), and trans-Golgi network 38 (TGN-38) (Affinity BioReagents, Inc., Golden, CO). Sytox Green nuclear stain, FITC-conjugated phalloidin, and anti-mouse and anti-fluorescein Alexa 488 amplification kits were purchased from Molecular Probes, Inc. Secondary antibodies and normal animal sera were purchased from Zymed Laboratories, Inc., Santa Cruz Biotechnology, Inc., and Jackson Immunoresearch Laboratories, Inc. (West Grove, PA).

Animals. Male Sprague-Dawley rats (250-350 g) were obtained from Harlan, Inc. (Indianapolis, IN) and received humane care according to guidelines prepared by the National Academy of Sciences and the National Institutes of Health. Rats were injected intraperitoneally 17 hours before use with 120 μg/kg CTX or 25 μg/kg PTX or solvent.[14] Other animals were given dibutyryl cAMP (30 mg/kg) intraperitonealy, either as a single injection 1 hour before use[20] or, to replicate the time period of toxin exposure, 5 injections administered at 4-hour intervals. Rats were injected intravenously with 70,000- or 10,000-d FITC-dextran or Texas red–dextran in saline 2 minutes to 15 hours before killing, as indicated in the text and figure legends. Liver weight was decreased by 13% to 27% ($P < .01$ to $P < .001$) by overnight exposure to cAMP and toxins, likely as a result of the catabolic effects of cAMP. Body weight was not affected by these agents, so quantitative data were normalized to per liver or per 100 g body weight.

Fractionation of Liver Vesicles. After rat treatment, livers were chilled by perfusion and homogenized in 5 volumes of ice-cold buffer (250 mmol/L sucrose, 3 mmol/L imidazole [pH 7.1]) with a Dounce homogenizer. Postnuclear supernatants (PNS) were prepared, 2.75 mL was layered over 36 mL of 30% Percoll (in a stock solution of 357 mmol/L sucrose, 2.86 mmol/L $CaCl_2$, 14.3 mmol/L HEPES [pH 7.2]) in 39 mL Quick-seal tubes and centrifuged at 48,300*g* for 45 minutes. Gradients were fractionated from the bottom into 30 1.25-mL fractions. Fractions were used fresh for acidification studies or were frozen for other assays.

Endosomes. Total liver populations of dextran-loaded endocytic vesicles were isolated from liver homogenates as a microsomal pellet as described,[5,14] resuspended in isotonic buffers containing 140 mmol/L K gluconate and 30 mmol/L Bis-Tris (pH 7.1), and kept at 4°C.

Vesicle Acidification. ATP-dependent acidification rates, steady-state ATP-dependent intravesicular pH (pH_i), proton efflux rates (normalized to the transmembrane H^+ gradient), and Na^+/H^+ exchange were measured in fresh endosomes or Percoll gradient fractions from changes in the ratio of fluorescein fluorescence.[5,14]

Analysis of FITC-Dextran in Gradient Fractions. Fluorescein fluorescence was measured in homogenates, PNS, or Percoll gradient fractions at 493 nm/530 nm. Intravesicular FITC-dextran was taken to be the difference in fluorescence measured in the absence or presence of 0.02% Triton-X 100 that was quenched by saturating amounts of anti-fluorescein antibody. Standard curves of FITC-dextran were used to convert fluorescence to nanograms of FITC-dextran. Preliminary studies showed intravesicular FITC-dextran was not caused by trapping of FITC-dextran during the homogenization step. The yield of intravesicular FITC-dextran was >95% complete (data not shown).

WGA Binding. To identify plasma membranes, livers were perfused at 4°C in a recirculating mode for 60 minutes with 10 mg FITC-WGA, followed by single-pass perfusion with buffer alone, similar to Bartles et al.[21] After fractionation on Percoll gradients, samples were centrifuged at 100,000*g* for 60 minutes to separate membrane-bound from supernatant (soluble) FITC-WGA, and fluorescein content was assessed fluorometrically. Membrane-bound FITC-WGA peaked in Percoll fractions 22-24 ($n = 3$), >95% of the fluorescence was located outside membrane vesicles, and no ATP-dependent acidification could be detected from internalized FITC-WGA (data not shown).

Plasma Concentration of Fluorescent Dextran. Plasma levels of FITC- and TR-dextrans were measured fluorometrically. Because plasma levels of 10,000-d dextrans fell rapidly as a result of renal excretion[22] (data not shown), 70,000-d dextrans were used for quantitative studies. Twenty minutes after injection of 100 mg 70,000-d FITC-dextran, plasma levels were 6.5 ± 0.8 mg/mL ($n = 24$). Fifteen hours after injection of 50 mg 10,000-d dextrans, plasma levels averaged 9 μg/mL ($n = 4$).

Enzyme Assays. *N*-Acetyl-β-glucosaminidase and β-glucuronidase were measured as described.[15] Alkaline phosphodiesterase I (APDE-I), a plasma membrane marker, was assayed from the appearance of *p*-nitrophenol (410 nm) in cuvettes containing 20 μg of protein in 1 mL 100 mmol/L Tris, 25 mmol/L $CaCl_2$ (pH 9.0), 2 mmol/L thymidine-5′-monophosphate-*p*-nitrophenyl ester, and 0.2% Triton X-100.[21,23,24] Specific activity was enriched in the peak gradient fraction (fraction 23) 10.0-fold (± 1.7; $n = 4$) compared with PNS.

Liver Fixation and Immunofluorescence. For confocal microscopy, we injected 10 to 25 mg per rat of 10,000-d TR-dextran as FITC fluorescence faded during antibody binding, and even only 5 to 10 mg of 70,000-d TR-dextran produced fluorescence so bright that cell architecture could not be analyzed. After treatment, livers were perfused via the portal vein with phosphate-buffered saline (PBS) and fixed by perfusion with 150 mL of 4% paraformaldehyde in PBS at 4°C. Livers were cut into 0.5-cm pieces, fixed for 2 hours in the same fixative, and infiltrated with sucrose by incubation for 30 minutes each in 5%, 10%, 12.5%, and 15% sucrose in PBS, all at 4°C. After overnight storage in 20% sucrose in PBS at 4°C, pieces were soaked in a mixture of 2:1 20% sucrose/PBS: OCT tissue freezing medium for 30 minutes at room temperature and frozen in a block of the same solution using isopentane chilled in liquid nitrogen and stored at −70°C until use. Cryostat sections (~20 μm) were rehydrated in PBS for 5 minutes, incubated 3×5 minutes in 50 mmol/L NH_4Cl in PBS, washed 3 times in PBS, and blocked for 30 minutes in PBS containing 0.2% Triton X-100 with 20% normal serum or 20% bovine serum albumin. Sections were incubated for 2 hours in primary antibody diluted in 0.2% Triton-X 100 in PBS with 2% serum, washed in PBS, incubated in secondary antibody diluted in 2% serum in PBS for 60 minutes, washed in PBS, and mounted with VectaShield. Alexa 488 amplification kits were used with EEA1 and transferrin receptor antibodies, according to the manufacturer's instructions. Other tissue sections were incubated with preimmune serum and secondary antibodies to confirm antibody specificity. Some sections were stained with Sytox Green nuclear stain after pretreatment with DNAase-free RNAase or stained with FITC-phalloidin according to the manufacturer's instructions.

Sections were imaged using a Bio-Rad MRC 600 confocal microscope (Hercules, CA). Images optically sectioned at 1 μm were cap-

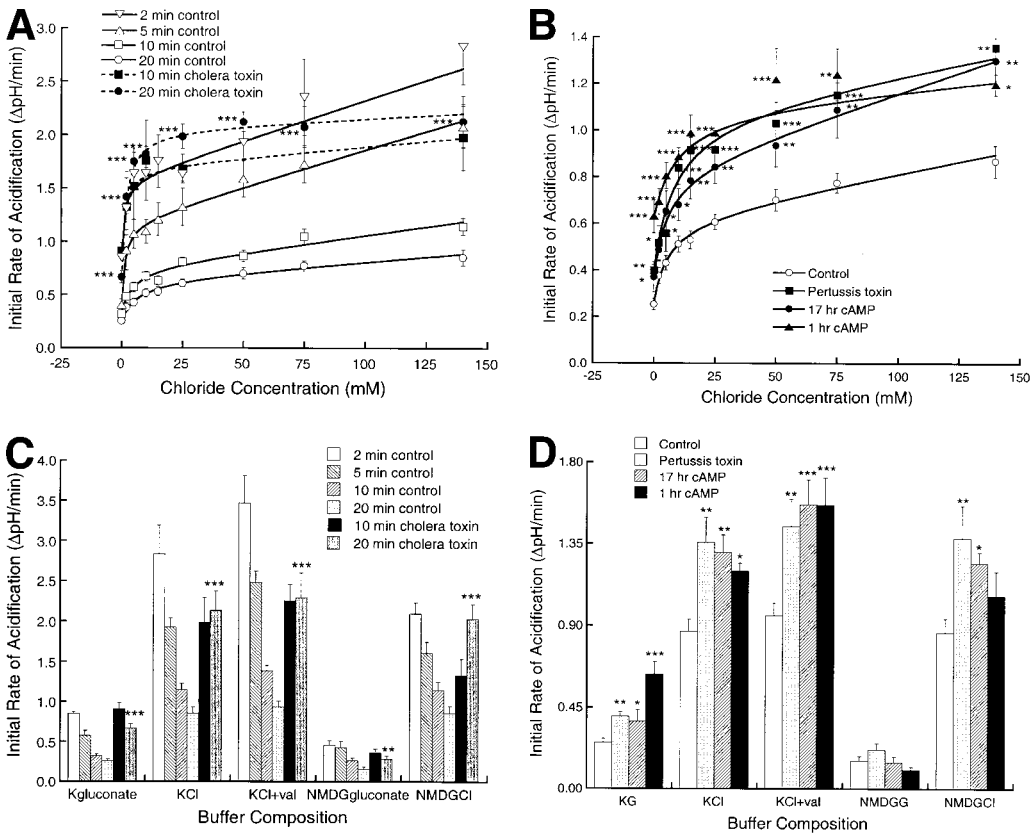

FIG. 1. Acidification rates of endosomes loaded for 2 to 20 minutes with 70,000-d FITC-dextran from control rats and rats treated with CTX (A, C), PTX (B, D), or dibutyryl cAMP (B, D). (A, B) Buffers contained 140 mmol/L K^+ and a mixture of Cl^- and gluconate. (C, D) Buffers contained 140 mmol/L of the indicated salt without or with 10 μmol/L valinomycin. (A, C) n = 4-59. (B, D) Time of endocytosis was 20 minutes (n = 4-17). $^*P < .05$; $^{**}P < .01$; $^{***}P < .001$, compared with control data.

tured and processed using Adobe Photoshop (Adobe Systems, Inc., San Jose, CA). Preliminary studies established that there was no significant "bleed-through" of fluorescence between any of the 3 channels used (green, red, and far-red) except for the very bright labeling of actin with FITC-phalloidin, which was faintly visible in the red channel. Under bright illumination, unstained liver exhibited punctate pericanalicular autofluorescence in all 3 channels, particularly after CTX treatment. These likely represented lipofuscin in lysosomes,[25] based on location, appearance, and colocalization with endocytosed dextran, but were not visible under the conditions used for this study.

Western Blotting. Sodium dodecyl sulfate–polyacrylamide gel electrophoresis was performed through 4% stacking and 7% or 12% running gels with equal amounts of protein in each lane. Proteins were transferred to nitrocellulose membranes electrophoretically, blots were washed in Tris-buffered saline with 0.3% Tween (TBST), blocked with 5% dry milk or 4% donkey serum, incubated with primary antibody for 2 or 3 hours, washed in TBST, incubated with secondary antibody conjugated to horseradish peroxidase, washed, and developed using chemiluminescence. Bands were captured on x-ray film.

Calculations and Statistics. For plots of acidification rates versus buffer Cl^- concentration, curves were fit to the data using nonlinear curve-fitting techniques and a form of the Michaelis-Menton equation ($y = ([ax]/[b + x]) + cx + d$) as described.[14,15] Data were presented as mean (±SEM for $n \geq 3$). Values were compared by the Student's t test, with $P < .05$ taken to indicate statistical significance.

RESULTS

Acidification of Early and Late Endosomes. In previous work, we showed that CTX and PTX increase endosome acidification rates and that different types of purified endocytic vesicles acidify at different rates.[14-16] Specifically, late endosomes (multivesicular bodies [MVB]) and lysosomes acidify more slowly than purified vesicles thought to represent earlier stages of endocytosis (CURL, compartment for uncoupling of receptor and ligand; and RRC, recycling receptor compartment vesicles). To extend these observations, we measured acidification rates in 4 temporally different populations of endosomes derived from the sinusoidal membrane that contained a pH-sensitive fluorescent probe of FPE. As livers were pulsed with equal amounts of the FPE probe, 70,000-d FITC-dextran and the total endosome population was studied, acidification rates reflected the algebraic sum of rates of all endocytic vesicles that internalized FITC-dextran during the duration of the pulse.

As shown in Fig. 1A and 1C, ATP-dependent initial rates of acidification progressively decreased as the age of the endosome population increased, regardless of the ion composition of the buffer, even when vesicle membrane potential was clamped by KCl + valinomycin. Because the main transporters responsible for liver endosome acidification appear to be the electrogenic vacuolar H^+-ATPase and a parallel Cl^- conductance,[4,14-17] nonlinear curve-fitting was used to estimate the parameters that best described the relationship between acidification rates and buffer Cl^- concentration (Fig. 1A).[5,14-17] This relationship was best described by the sum of an apparently saturable component, a linear component, and a constant rate, $y = ax/(b + x) + cx + d$, where "a" represents the maximum acidification rate as a result of Cl^- ($V_{max\ Cl-}$); "b" is the estimated dose for 50% maximum rate (ED_{50}) for Cl^-; "c" is the constant for a linear increase in rate related to Cl^- (V_{linear}); and "d" is the rate in the absence of Cl^- ($V_{0\ Cl-}$). Best estimates for these constants, along with the errors in estimating them and the calculated acidification rate at 140 mmol/L Cl^-, are shown in Table 1. The ED_{50} for Cl^- increased with endosome age, whereas all 3 rate terms decreased, result-

TABLE 1. Kinetic Rate Constants for Endosome Acidification Rates (V) Plotted vs. Cl^- Concentration and Steady-State ATP-Dependent pH_i

Treatment	FITC-Dextran Pulse (min)	$V_{max\ Cl^-}$ (ΔpH/min) Parameter A	ED_{50} Cl^- (mM) Parameter B	V_{linear} (ΔpH/min) Parameter C	$V_{0\ Cl^-}$ (ΔpH/min) Parameter D	Total V at 140 mmol/L Cl^- (ΔpH/min) (Calculated)	Steady-State pH_i (140 mmol/L KCl)
Control	2	0.73 ± 0.10	1.1 ± 0.6	0.0075 ± 0.003	0.85 ± 0.03	2.63	5.74
	5	0.77 ± 0.17	1.3 ± 1.6	0.0069 ± 0.002	0.40 ± 0.06	2.14	5.76
	10	0.44 ± 0.07	4.3 ± 2.1	0.0032 ± 0.001	0.32 ± 0.02	1.19	6.08
	20	0.38 ± 0.09	6.5 ± 3.9	0.0019 ± 0.001	0.26 ± 0.03	0.88	6.12
CTX (17 hours)	10	0.79 ± 0.25	1.6 ± 2.6	0.002 ± 0.003	0.91 ± 0.08	1.97	5.86
CTX (17 hours)	20	1.39 ± 0.17	1.8 ± 1.1	0.0011 ± 0.002	0.67 ± 0.06	2.20	5.72
PTX (17 hours)	20	0.69 ± 0.21	8.6 ± 5.7	0.0019 ± 0.002	0.40 ± 0.03	1.31	6.03
cAMP (1 hour)	20	0.48 ± 0.11	9.7 ± 7.9	0.001 ± 0.001	0.63 ± 0.06	1.21	6.09
cAMP (17 hours)	20	0.47 ± 0.13	5.5 ± 4.7	0.003 ± 0.001	0.36 ± 0.06	1.30	5.98

NOTE. Parameters were estimated by nonlinear curve-fitting for the equation $y = ax/(b + x) + cx + d$. Values for estimated parameters are given ± the calculated errors in fitting parameters to the data.

ing in a progressively decreasing calculated total rate. In parallel, the steady-state pH_i became more alkaline (Table 1).

CTX and PTX, Dibutyryl cAMP, and Acidification. Endosomes from CTX-treated livers pulsed with FITC-dextran for either 10 or 20 minutes exhibited acidification rates similar to or even faster than those of endosomes from control livers that were pulsed with FITC-dextran for only 2 or 5 minutes (Fig. 1A and 1C). These observations were consistent, regardless of buffer ion composition, and were both reflected by changes in all kinetic parameters (Table 1); and associated with more acid steady-state pH_i (Table 1).[14] PTX and both overnight (17 hours) and short-term (1 hour) dibutyryl cAMP administration caused changes in the rate parameters of endosome acidification that were qualitatively similar to the effects of CTX, although the changes were not as great and neither altered the $ED_{50\ Cl-}$ (Fig. 1B and 1D; Table 1).

We also confirmed that CTX and PTX as well as 17-hour exposure to dibutyryl cAMP increased Na^+/H^+ exchange (an early endosome marker[5]) in 20-minute endosomes (CTX > PTX, 17-hour dibutyryl cAMP > control), but did not alter proton efflux rates in the absence of Na^+ (data not shown). Because steady-state pH_i reflects a balance between proton influx, proton buffering, and proton efflux,[15-17] these changes in steady-state pH_i (Table 1) suggested that proton influx was the dominant factor in determining pH_i.

Collectively, these findings confirmed our earlier observation that CTX, PTX, and dibutyryl cAMP increase acidification rates of endosomes,[14] and extended them to show that these agents similarly altered the kinetic parameters of acidification rates of older endosomes to more closely resemble the kinetic parameters of earlier endosomes from control livers, and that cAMP had similar effects when administered *in vivo* for 1 or 17 hours. Because cAMP and the toxins appeared to block "age"-related changes in endosome ion transport, these findings suggested that these agents altered critical step(s) in the maturation and/or remodeling of endosomes.

FPE. To determine whether CTX also altered the distribution of endocytosed cargo between early endosomes and late endosomes or lysosomes, and to assess changes in net FPE, livers were pulsed with FITC-dextran and fractionated on self-generated Percoll gradients. The time courses of uptake and distribution of FITC-dextran in control livers are shown by the open circles in Fig. 2. Intravesicular FITC-dextran first entered low-density (~1.04-1.06 g/mL) vesicles in fractions ~20-27. By 10 minutes, some probe had appeared in dense vesicles (~1.07-1.13 g/mL) in fractions ~2-6. With time, the amount of probe in low-density endosome fractions achieved an approximate steady-state content, whereas the amount in dense vesicles continued to increase. After an overnight pulse-chase with 10,000-d FITC-dextran, a smaller probe rapidly cleared from blood, virtually all the probe was found in dense vesicles in fractions ~1-5 (Fig. 3A). Protein content (Fig. 3B) was greatest in fractions at the bottom of the gradient (fractions ~1-5) and at the top (fractions ~28-30), where cytosolic proteins and >92% of soluble extravesicular FITC-dextran were located.

We employed measurements of marker enzymes (Fig. 3C and 3D) and Western blotting for marker proteins (data not shown) to determine the position on these gradients of plasma membranes and various organelles. Plasma membranes were found in a subset of low-density fractions (fractions ~22-24), as indicated by the distribution of the marker enzyme, APDE-I (Fig. 3C), and FITC-WGA. By contrast, the canalicular membrane protein, MRP-2,[26] was distributed in denser fractions (~16-22) (data not shown). This was unexpected because APDE-I is thought to be located principally on canalicular membranes, and canalicular membranes are thought to be less dense than basolateral membranes.[21,23]

Transferrin receptor, thought to be a marker of early endosomes and plasma membranes, was found only in fractions 22-26, where it overlapped with both (Figs. 2A, 2B, 3C). EEA1, a cytoplasmic protein that binds to early endosomes,[27] was identified in fractions 20-26 (overlapping with endosomes) and in cytosol in fractions 28-30. TGN vesicles, identified by large amounts of the resident protein, TGN-38,[28] were located principally in fractions ~20-22, although some of the TGN-38 in these fractions was likely located on the plasma membrane and in endosomes.[28]

The dense peak of endocytosed FITC-dextran found in fractions ~2-6 (Figs. 2 and 3A) likely corresponded to dense late endosomes and/or lysosomes as reflected by the sequential time course of FITC-dextran distribution (Figs. 2 and 3A) and distribution of the lysosomal marker enzymes, *N*-acetyl-β-glucosaminidase and β-glucuronidase (Fig 3D). LAMP-1[29] was localized to fractions 3-6 (data not shown), which likely contain late endosomes/less-mature lysosomes, but not to fractions 1 and 2, which probably represented a kinetically deep compartment of old lysosomes.

CTX had no effect on the density distribution or content of any of these markers (Fig. 3; data not shown). CTX decreased the protein content of fractions 3-4 (Fig. 3B) ($P < .05$), likely as a result of accelerated catabolism and autophagy. After just

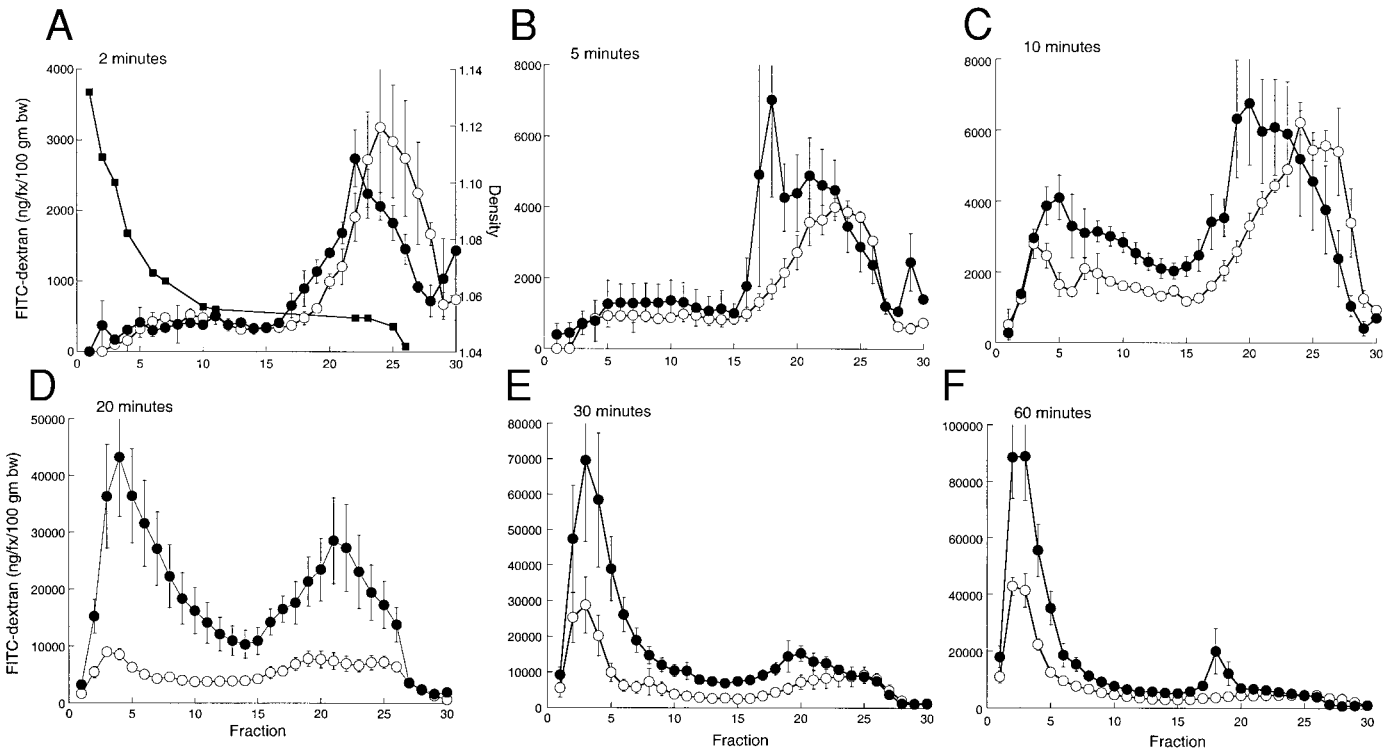

FIG. 2. Effect of CTX on content and distribution of endocytosed FITC-dextran in rat liver. (■), Position of density-marker beads (A). Control (○) and CTX-treated (●) rats were given 100 mg 70,000-d FITC-dextran intravenously for the indicated times (n = 3-9).

2 minutes of uptake, liver content of endocytosed FITC-dextran did not differ between control and CTX-treated liver, suggesting that the initial rate of FPE was not greatly altered (Fig. 2A). However, CTX-treated livers contained much more FITC-dextran than control livers at uptake periods of 5 minutes to 60 minutes, and this increased amount of probe was found in both endosome and lysosome peaks. By contrast, after a pulse and overnight chase, the total amount of endocytosed FITC-dextran was similar in both control and CTX-treated livers, as was the amount of probe retained in lysosomal fractions (Fig. 3A).

To further examine the effects of CTX on liver content of endocytosed probe, the amount of intravesicular FITC-dextran in fractions 1-30 was summed for each liver in Fig. 2 (Fig. 4). FITC-dextran content was greater in CTX-exposed livers at all time points after 2 minutes and was significantly greater at 20, 30, and 60 minutes. Similar results were obtained when intravesicular FITC-dextran was measured directly in samples of whole-liver homogenate or in the PNS (data not shown).

To assess the rate of transfer of endocytosed dextran from low-density endosomes to high-density lysosomes, changes in the endosome and lysosome pools over time were examined. For each time point, the mean sum of FITC-dextran in Percoll gradient fractions was calculated for fractions 1-10 and for fractions 11-30, representing the lysosome and endosome pools, respectively. As shown in Fig. 4, lysosome content of FITC-dextran (which presumably reflected primarily input from the endosome pool, as losses to bile were likely to be small) increased with time in approximately parallel patterns in both control and CTX-treated livers, suggesting similar rates of transfer from endosomes to lysosomes. Because the endosome pools were larger in CTX-treated livers, the fractional transfer of the endosome pool to the lysosome pool also was calculated for each time interval. Control and CTX-treated livers exhibited no consistent differences in the fractional transfer of probe from endosomes to lysosomes (data not shown). Thus, CTX appeared to have no effect on initial rate of probe uptake or transfer of probe to lysosomes, but greatly increased liver content of probe in both endosomes and lysosomes, best explained by a decrease in diacytosis. Both PTX and dibutyryl cAMP also increased net FPE and the amount of endocytosed probe in both endosomal and lysosomal fractions after a 20-minute pulse of FITC-dextran (Fig. 5), although the effects of CTX were quantitatively greater (Fig. 2D).

CTX also appeared to shift the density of endosomes. At least at early time points (2-10 minutes), considerable FITC-dextran in CTX-exposed livers was found in fractions ~17-20, more dense than plasma membranes, whereas in control livers, FITC-dextran was in fractions ~23-27, less dense than plasma membranes (Figs. 2A-2C, 3C). Because of these changes, we also examined the distribution of 2 rab proteins thought to be associated with early (rab 5) and late (rab 7) endosomes.[30] These proteins were identified in a wide range of fractions (primarily ~8-26 for rab 5 and ~8-12 and ~18-26 for rab 7), suggesting that they were associated with vesicles of a wide range of densities, including vesicles that did not enclose much FITC-dextran. CTX had no apparent effect on the amount or distribution of either rab 5 or rab 7 (data not shown).

Acidification of Endosomes in Percoll Gradient Fractions. Neither Cl^- nor CTX altered acidification rates of dense vesicles in fractions 2-8 (Fig. 6), consistent with our findings that lysosome acidification is only modestly affected by Cl^-,[15] and that CTX has little effect on acidification of purified lyso-

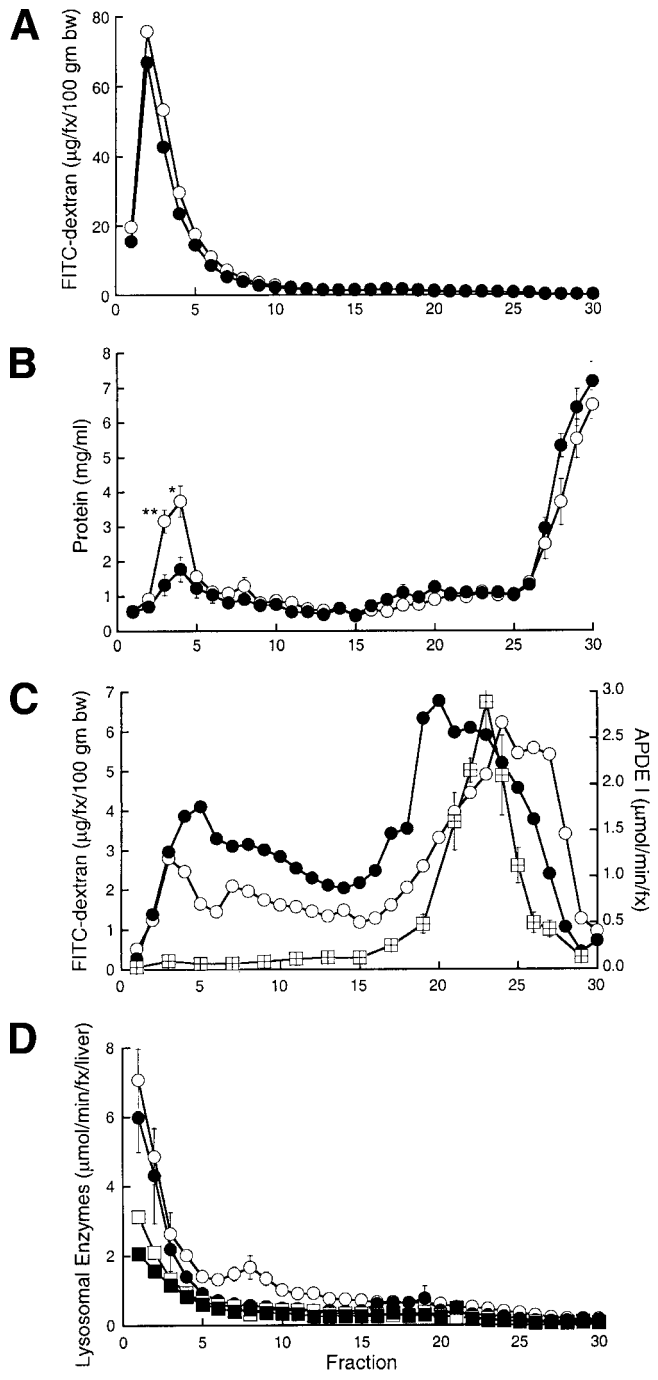

FIG. 3. Location of overnight chased FITC-dextran, protein content, and organelles on Percoll gradients in control (○, □) and CTX-treated (●, ■) liver. (A) FITC-dextran (50 mg 10,000 d) given intravenously 17 hours before liver fractionation (n = 2). (B) Protein content (n = 9). $*P < .01$, $**P < .001$. (C) APDE-I (⊞) (n = 4) and FITC-dextran (○, ●) endocytosed for 10 minutes (from Fig. 2C). (D) Lysosomal enzymes: *N*-acetyl-β-glucosaminidase, ○, ● (n = 3); β-glucuronidase, □, ■ (n = 2).

somes.[31] Acidification rates of vesicles in all endosome fractions (fractions ~15-27) were increased after CTX exposure in the presence and absence of Cl^-. These differences were greatest in fractions ~15-20, the population of endosomes density-shifted by CTX. These findings suggest that CTX affected many types of endosomes, but the greatest effect was on endosomes in fractions ~15-20.

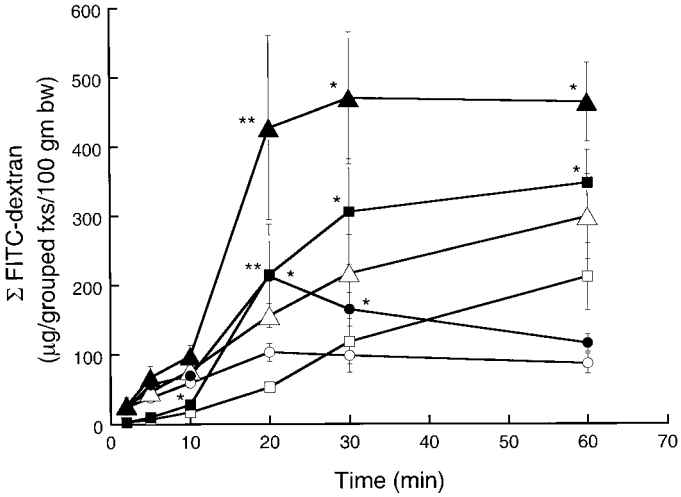

FIG. 4. Summed content of intravesicular FITC-dextran in Percoll gradient fractions 11-30 (endosomes, circles), fractions 1-10 (lysosomes, ○, ●) and in all 30 Percoll gradient fractions (△, ▲) in control (*open symbols*) and CTX-treated (*closed symbols*) livers. Values are mean ± SEM from 3-9 livers. $*P < .05$, $**P < .01$ compared with control. (○), Control fx 11-30; (□), control 1-10; (△), control all fx; (●), CTX fx 11-30; (■), CTX fx 1-10; (▲), CTX all fx.

Microscopic Localization of Endocytic Vesicles. To further assess trafficking and distribution of endocytosed FPE probe in polarized rat hepatocytes, confocal microscopy was used to examine cryostat sections of rat livers. After 20 minutes of endocytosis in control liver (Fig. 7), punctate red fluorescence was visible at both the sinusoidal membrane and in a pericanalicular location. Immunofluorescent staining for MRP-2[26] (Fig. 7A) marked the canalicular membrane. TGN-38 was localized to separate vesicular structures in the pericanalicular region that did not colocalize with TR-dextran (Fig. 7A and 7C). FITC-phalloidin identified actin bands located immediately under both sinusoidal and canalicular membranes (Fig. 7E). No TR-dextran–containing vesicles were seen near the nucleus, delineated by the nuclear stain Sytox Green (Fig. 7G). Some TR-containing vesicles were also observed outside

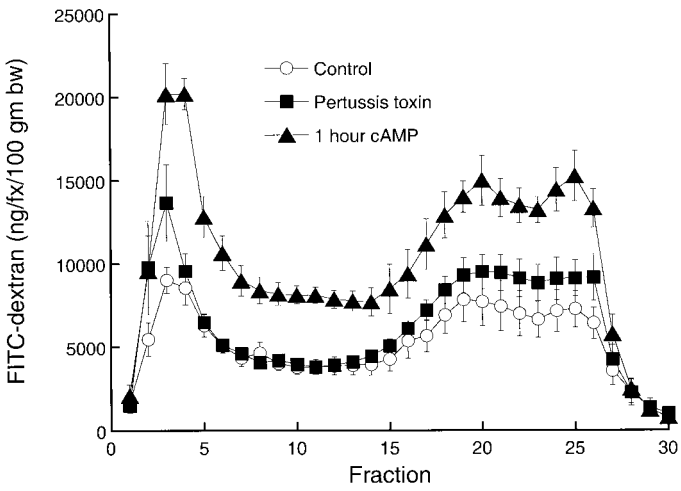

FIG. 5. Effect of exposure *in vivo* to PTX and dibutyryl cAMP on distribution of FITC-dextran on Percoll gradients 20 minutes after intravenous injection of 100 mg 70,000-d FITC-dextran. (○), control livers (n = 9); (■), PTX (n = 4); (▲), cAMP (n = 5). Values are mean ± SEM.

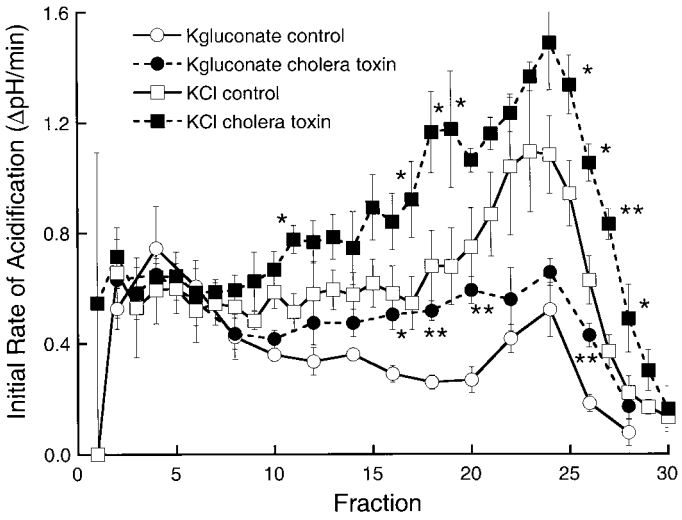

FIG. 6. ATP-dependent acidification rates of vesicles, loaded for 20 minutes with 70,000-d FITC-dextran, in Percoll gradient fractions from control (○, □; n = 4) and CTX-treated (●, ■; n = 3) livers assayed in 140 mmol/L K gluconate (○, ●) or KCl (□, ■) buffers. Values are the mean ± SEM. $*P < .05$, $**P < .01$ compared with control.

the hepatocyte basolateral membrane, presumably in endothelial and Kupffer cells; however, FPE could not be assessed in nonparenchymal cells because of their small size, low prevalence, and irregular geometry.

Effect of CTX on Endosome Location. The number and distribution of punctate TR-dextran–containing vesicular structures was considerably altered by CTX. First, vesicles appeared more numerous and more brightly fluorescent, although these aspects could not be quantitated reliably. Readily apparent on all images was the more random distribution of punctate TR-dextran fluorescence throughout the hepatocyte cytoplasm and the appearance of large novel perinuclear collections of TR-dextran–labeled vesicles (Fig. 7B, 7D, 7F, 7H). CTX also appeared to redistribute elements of the TGN to a perinuclear position; however, TGN-38–labeled vesicles did not colocalize with TR-dextran (Fig. 7D). Z series of images were obtained through the entire height of hepatocytes from both control and CTX-treated livers stained with MRP-2 antibody to confirm that the perinuclear collections of vesicles were not clusters of pericanalicular vesicles that appeared near the nucleus because of artifacts of optical sectioning.

Endosome/Lysosome Markers. Additional antibodies were used to determine the location of markers of early or recycling endosomes (EEA1 and transferrin receptor[32]) and of late endosomes/lysosomes (LAMP-1)[29] (Figs. 8 and 9). In control liver, punctate staining for EEA1 was localized immediately under both sinusoidal and canalicular membranes (Fig. 8A), more prominently the latter, consistent with both membranes as sites of endocytosis.[33] Some TR-dextran–containing vesicles appeared to colocalize with EEA1 as shown by yellow vesicles. Antibodies to the transferrin receptor yielded low levels of diffuse staining along sinusoidal membranes and intensely stained punctate vesicular structures in the pericanalicular area (Fig. 9B). Near the canaliculus, only a few transferrin receptor–positive vesicles colocalized with TR-dextran–positive vesicles, possibly representing recycling endosomes, while most transferrin receptor–positive vesicles closely resembled TGN vesicles (Fig. 7A and 7C). In CTX-treated livers, EEA1 and transferrin receptors were identified in the same locations as in control livers; however, additional regions of staining for both antibodies colocalized with TR-dextran–positive vesicles in perinuclear clusters (Figs. 8B, 9D-9F). These double-labeled vesicles may represent mistrafficked early/recycling endosomes.

In control livers, LAMP-1 localized to punctate structures in the pericanalicular region (Fig. 8C) and in sinusoidal endothelial cells, locations consistent with its presence in late endosomes/lysosomes.[29] In these locations, LAMP-1 colocalized virtually completely with TR-dextran–containing vesicles, as shown by the yellow color of merged images. In CTX-treated livers, LAMP-1 colocalized with both pericanalicular vesicles and with some perinuclear TR-dextran–containing vesicles (Fig. 8D). The latter may represent mistrafficked late endosomes/lysosomes.

Time Course of Endosome Localization. To examine spatial aspects of trafficking kinetics of FP endosomes, livers were administered TR-dextran for 2, 4, 6, 10, and 20 minutes and for 15 hours. Sections were stained for MRP-2 to identify the bile canaliculus. In control liver (Fig. 10A, 10C, 10E, 10G, 10I), TR-dextran first appeared in punctate structures immediately under the sinusoidal membrane. Over the next 4 to 8 minutes, TR-dextran–containing vesicles appeared to travel to and accumulate at the pericanalicular area. Transfer of endosomes from sinusoidal to canalicular regions was rapid, because by 4 minutes after dextran injection (data not shown), some labeled vesicles already were present in the pericanalicular space. Fifteen hours after administration of TR-dextran, probe was seen only in pericanalicular vesicles (Fig. 10I) that likely corresponded to the dense vesicles on Percoll gradients (Fig. 3A). Overall, the data in Figs. 7-10 suggested that hepatocytes took up probe from blood into early endosomes, which were located immediately under the sinusoidal membrane and a band of actin filaments in an area also occupied by EEA1. Shortly thereafter, vesicles rapidly trafficked to the pericanalicular space where many subsequently matured into LAMP-1–positive late endosomes and lysosomes. Some of the pericanalicular vesicles may be recycling endosomes destined to traffic back to the sinusoidal membrane. This pericanalicular area also contained EEA1, likely representing endocytosis from the canaliculus, and elements of the TGN.

Effect of CTX on Time Course. CTX treatment did not alter the sequential appearance of perisinusoidal and pericanalicular TR-dextran–loaded vesicles (Fig. 10B, 10D, 10F, 10H, 10J). However, as early as 2 minutes after injection, an occasional TR-dextran–positive vesicle was seen near the canaliculus, and by 4 minutes (data not shown), vesicles also were found randomly distributed throughout the hepatocyte cytoplasm. Furthermore, TR-dextran–containing vesicles began to appear near the nucleus as early as 4 to 6 minutes. These tightly packed aggregates of perinuclear vesicles persisted, even after an overnight pulse/chase.

PTX, Dibutyryl cAMP, and Endosome Localization. Exposure for 17 hours to either dibutyryl cAMP or PTX resulted in a distribution of vesicles, including the appearance of perinuclear clusters of vesicles, similar to that caused by CTX (data not shown). However, mislocalized perinuclear endosomes were not seen after just 1 hour of cAMP (data not shown), suggesting that this effect required prolonged exposure to cAMP. Altered trafficking to the perinuclear region was not

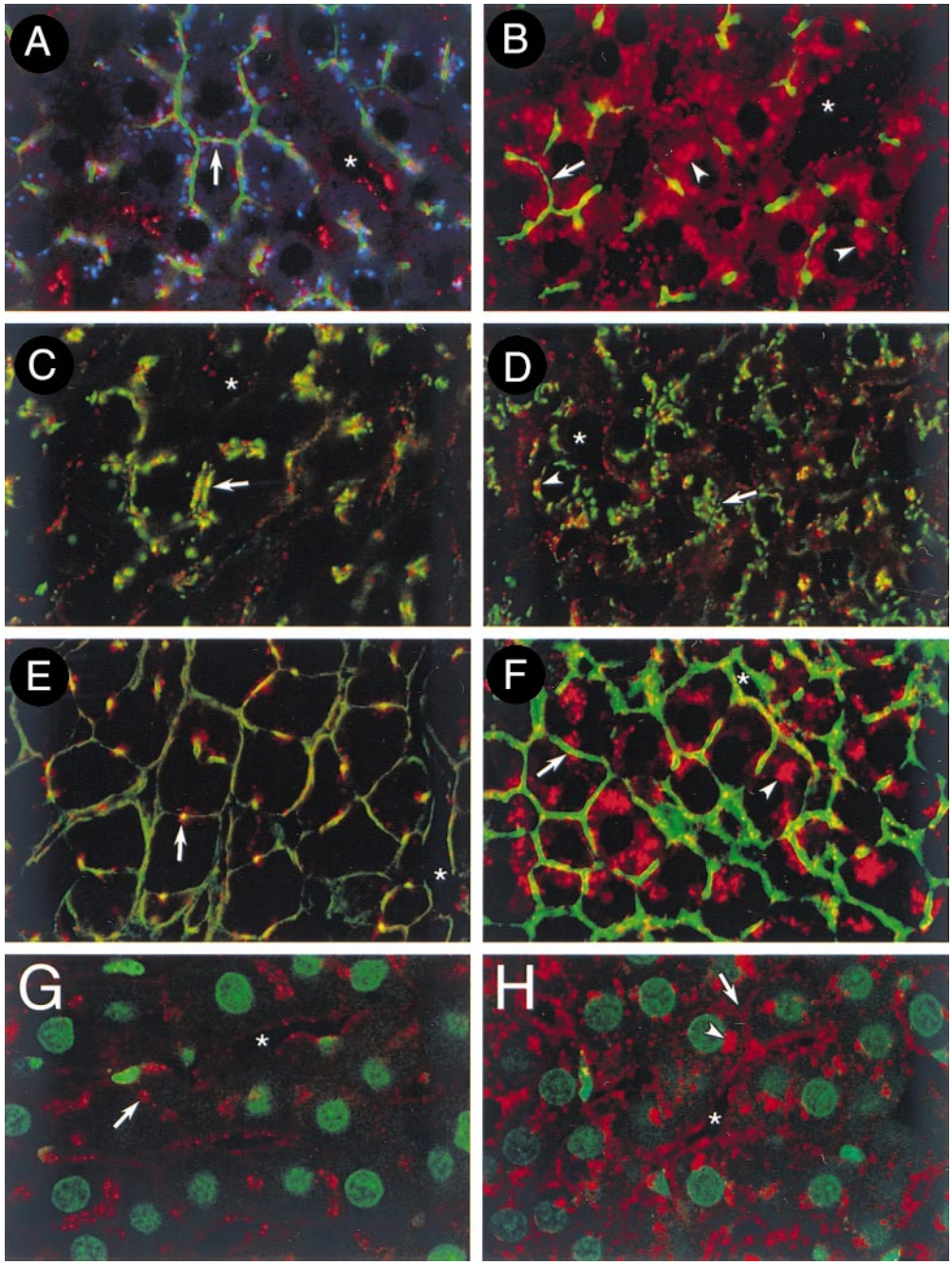

FIG. 7. Distribution of endocytic vesicles in relation to other cell structures. Control (A, C, E, G) and CTX-treated (B, D, F, H) livers were pulsed *in vivo* for 20 minutes with 10,000-d TR-dextran (*red*) and stained (*green*) with antibodies to MRP-2 (A, B) or TGN-38 (C, D) or treated with FITC-phalloidin (E, F) or the nuclear stain, Sytox Green (G, H). In (A), TGN-38 is *blue*. *Asterisks* indicate the hepatic sinusoid, *arrows* the bile canaliculus, and *arrowheads* perinuclear vesicles. Images representative of 7 to 104 images obtained from 1 to 6 livers each.

the result of elimination of microtubules, because colchicine prevented endosomes leaving the perisinusoidal region (data not shown).

Although fasting is reported to alter liver cAMP and endocytosis[18,34,35] and CTX-treated rats might not eat normally, as assessed by changes in endosome acidification, uptake, and distribution of probe on Percoll gradients and by confocal microscopy, CTX had similar effects on fed and fasted rats[18] (data not shown).

DISCUSSION

It is generally accepted that many fusion, remodeling, and budding steps occur during endocytosis, associated with sorting of endosome contents and receptors, as well as physical movement of vesicles to specific parts of the cell. Less is known about trafficking and regulation of vesicle ion transporters or their functional implications. Heterotrimeric G proteins and/or cAMP appear to affect a number of processes involved in endocytic vesicle trafficking,[8-11] including in liver stimulation of exocytotic insertion of transporters into apical and basolateral membranes.[12,13,36,37] However, it is not known whether either heterotrimeric G proteins and/or cAMP affect more general pathways of liver vesicular transport such as FPE. Based on prior work,[5,14-16] we hypothesize that ion transporters are added to/removed from vesicles during endosome maturation, and that heterotrimeric G proteins (G_s and G_{i2-3}), through cAMP, not other G protein effectors, increase endosome acidification by altering endosome remodeling, maturation, and/or trafficking, rather than through direct regulation of the vacuolar H^+-ATPase. If so, cAMP might be expected to alter FPE.

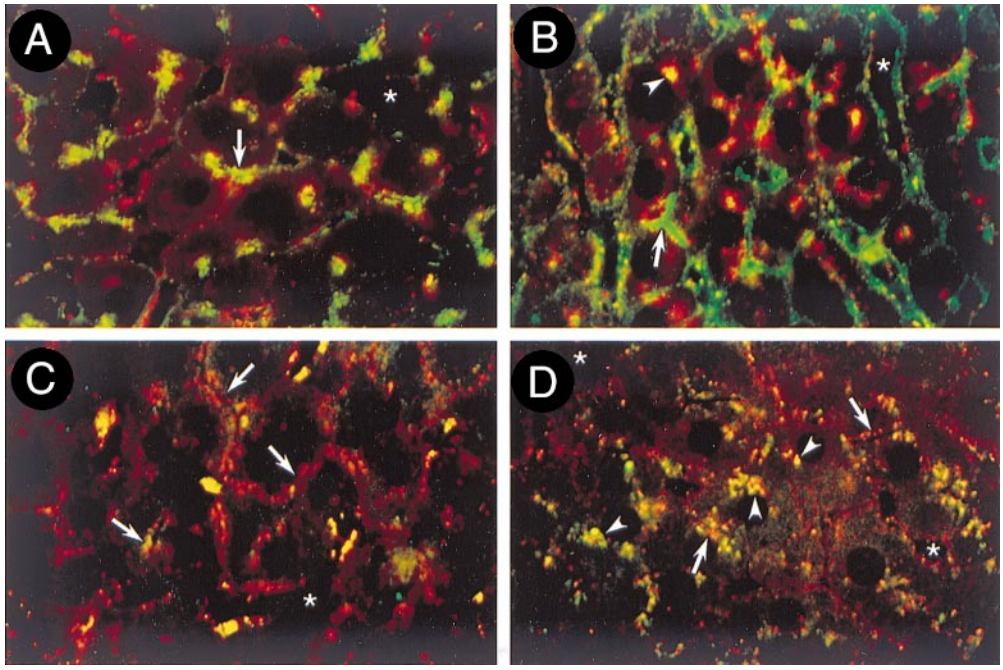

FIG. 8. Merged images showing the locations and areas of colocalization of endocytic vesicles (*red*) and EEA1 (*green*) (A, B) or LAMP-1 (*green*) (C, D) in control (A, C) and CTX-treated (B, D) livers pulsed with TR-dextran for 20 minutes. *Asterisks* indicate the hepatocyte sinusoids, *arrows* the bile canaliculus, and *arrowheads* perinuclear vesicles. Images representative of 32 to 45 images obtained from 3 livers each.

We chose to examine endosome populations loaded with a fluid-phase probe for different time periods. Although heterogeneous, these populations offer a global view of basolateral endocytosis and, as all vesicles were prepared in the same model system, differences in their properties should result solely from differences in endosome fusion/remodeling/trafficking. However, it is possible that subsets of basolateral endosomes exist that respond differently to maturation, toxins, and cAMP.

In control liver, we confirmed a progressive decline in rates of acidification with endosome "age," consistent with our prior findings that purified rat liver mid- and late endosomes and lysosomes acidified at slower rates than early endosomes.[15,16] Indeed, the kinetic parameters of 10- and 20-minute endosomes (Table 1) closely resembled those of CURL and MVB vesicles, respectively.[16] From these data alone, it is not possible to determine whether differences in acidification rates reflected changes in the turnover rate of the vacuolar H^+-ATPase or in endosome remodeling and the numerical density of pumps per vesicle or vesicle surface-to-volume ratio.

CTX, PTX, and cAMP all appeared to block or reverse this "age"-related change in endosome (but not lysosome [Fig. 6])[31] acidification (Fig. 1, Table 1), consistent with our prior findings that CTX caused smaller increases in acidifica-

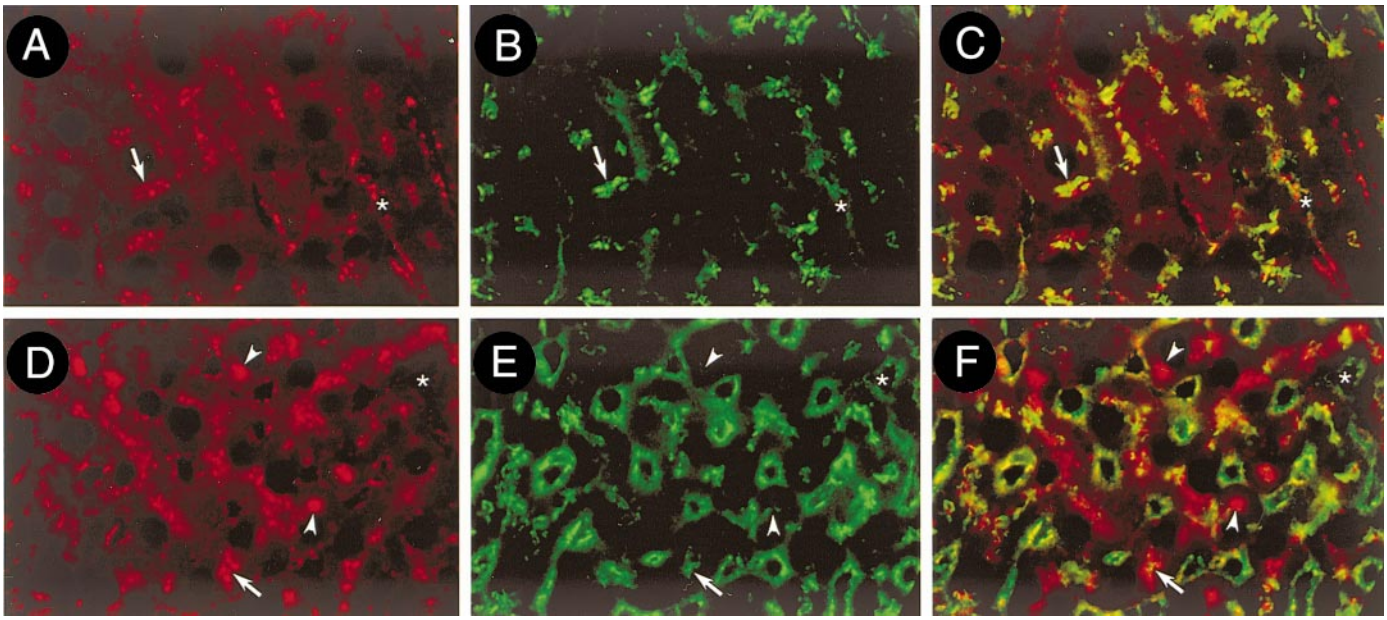

FIG. 9. Location of endocytic vesicles (*red*) and transferrin receptor (*green*) in control (A-C) and CTX-treated (D-F) livers pulsed with TR-dextran for 20 minutes. (C and F) are the merged images of (A, B) and (D, E), respectively. *Asterisks* indicate the hepatic sinusoids, *arrows* the bile canaliculus, and *arrowheads* perinuclear vesicles. Images representative of 21 to 31 images obtained from 3 livers each.

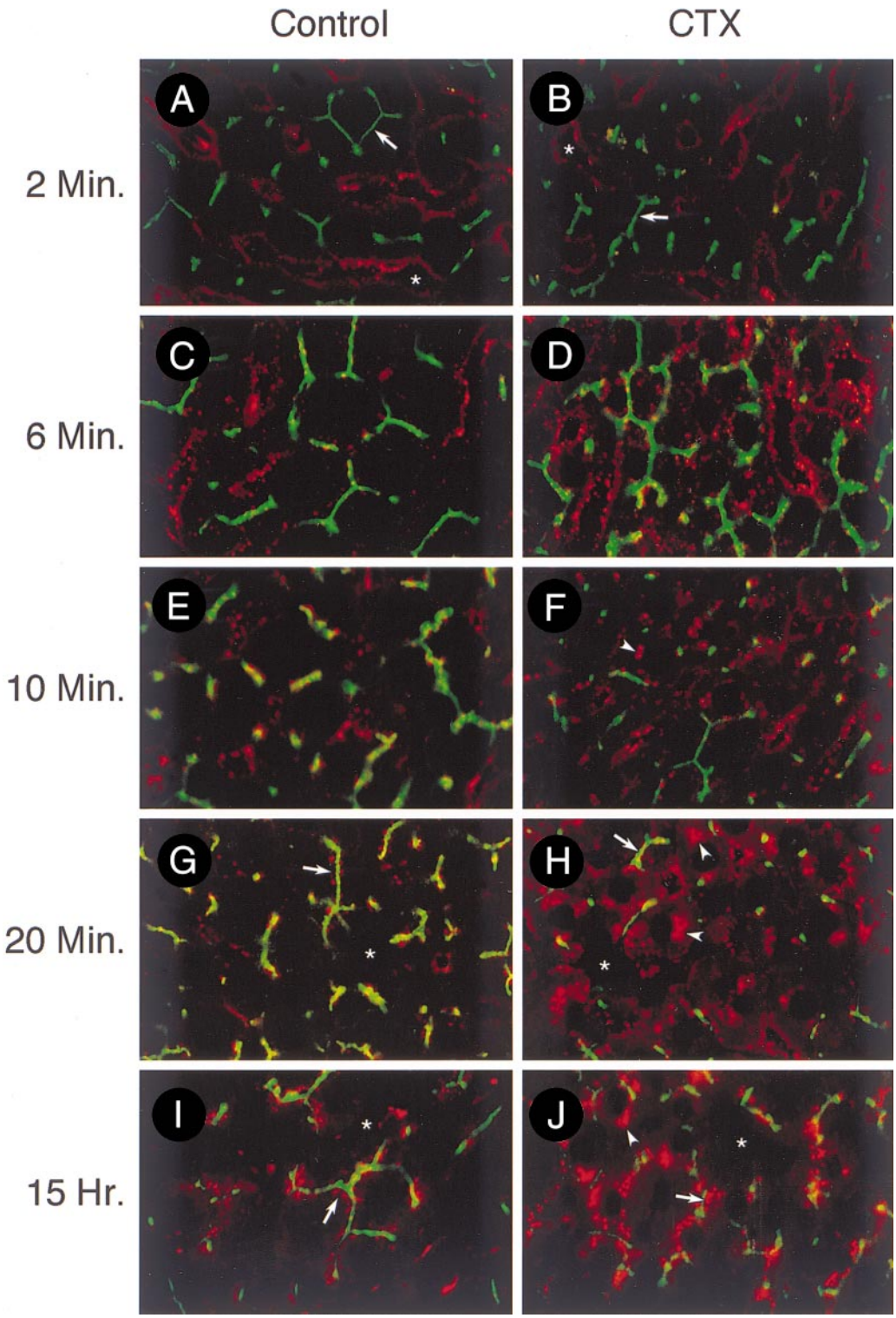

FIG. 10. Time course of distribution of fluid-phase endocytic vesicles in control (A, C, E, G, I) and CTX-treated (B, D, F, H, J) liver. Livers were pulsed with TR-dextran (*red*) for the indicated times, and sections were stained with antibody to MRP-2 (*green*). (A, B) Two minutes; (C, D) 6 minutes; (E, F) 10 minutes; (G, H) 20 minutes; (I, J) overnight. *Asterisks* indicate the hepatic sinusoids, *arrows* the bile canaliculus, and *arrowheads* perinuclear vesicles. Images representative of 12 to 104 images obtained from 1 to 6 livers each.

tion rates of early 2-minute endosomes than of later endosomes.[14] Two observations suggest these changes occurred because of altered endosome remodeling/maturation: 1) CTX, PTX, and cAMP also increased Na^+/H^+ exchange[14]; and 2) CTX, PTX, and cAMP *in vivo* (Fig. 1) increased endosome acidification much more than cAMP or protein kinase A added to isolated endosomes.[38]

To explore whether CTX, PTX, and cAMP caused quantitative and/or spatial changes in liver FPE, we fractionated liver on density gradients and employed confocal microscopy. Liver contains not only hepatocytes, but also nonparenchymal cells, all capable of FPE.[39] However, hepatocytes are more numerous, larger, and have a greater membrane surface area than nonparenchymal cells,[39,40] and when FPE is calculated per gram of liver, hepatocytes account for >50% to 73% of liver FPE. Thus, most of the internalized probe in Figs. 2-4 was likely in hepatocytes, an assumption supported by microscopic studies (Figs. 7-10).

The time course and distribution of endocytosed probe shown in Fig. 2 was similar to studies in other cell types.[6,24] We evaluated 6 time points to allow kinetic analysis of probe uptake and transfer. The pool of probe in endosome fractions reached an approximate steady-state after about 20 minutes, presumably reflecting a balance between endocytic uptake and losses as a result of transcytosis to bile, transfer to dense late endosomes/lysosomes, and efflux back to blood. As expected during continuous endocytosis, lysosome pool size continued to increase at all time points through 60 minutes.

CTX and, to a lesser degree, PTX and dibutyryl cAMP, increased liver content of probe in both endosome and lysosome fractions at 5- to 60-minute time points, suggesting that these agents increased initial rates of FPE and/or decreased probe efflux. Because both control and CTX-treated livers took up the same amount of FITC-dextran in 2 minutes (Fig. 2A), the former option is unlikely. A large fraction of internalized FPE probes (80% in cultured hepatocytes) are rapidly returned to the external environment by diacytosis.[41,42] It is likely, therefore, that CTX reduced the rate of diacytosis. Indeed, the unique higher density rapidly acidifying endosomes in gradient fractions ~15-20 (Figs. 2 and 6) might represent blocked diacytotic vesicles. If so, this appears paradoxical, because acute exposure to cAMP *in vitro* increases: 1) exocytotic insertion of intracellular vesicles containing Ntcp into the basolateral membrane[12]; 2) exocytotic insertion of organic anion transporters into the canalicular membrane[13,36]; and 3) biliary release of previously endocytosed horseradish peroxidase.[37]

Transfer of probe from endosomes to lysosomes did not appear to be greatly altered by CTX, because: 1) probe content in both endosomes and lysosomes was increased (Fig. 2); 2) probe in lysosome fractions rose with time in parallel in both control and CTX-treated livers (Fig. 4); and 3) the relative fractional transfer of probe from endosome to lysosome pools was similar for control and CTX-treated livers. However, CTX also may have increased the rate of loss of probe from lysosomes, because after overnight uptake, the lysosomal pool of dextran was similar in control and CTX-treated livers (Figs. 3A, 2F). This could occur if the slow transfer of lysosomal contents to bile (4%-5% per day)[37,43] were accelerated by CTX and/or cAMP.

Confocal microscopic studies of liver endocytosis characterized the normal spatial distribution of FP endosomes. After formation at the sinusoidal membrane, these vesicles appeared to traffic rapidly and efficiently to the pericanalicular region. Indeed, in examining many images, labeled vesicles were rarely seen in other regions. Microtubule-mediated translocation is likely responsible for this rapid trafficking, because: 1) hepatocytes exhibit a pericanalicular microtubule organizing center[44]; 2) in cultured hepatocytes, colchicine increases uptake of FPE probe into a small, rapidly recycling, endosome pool and decreases the cellular content of probe[41]; and 3) we observed that colchicine blocked all sinusoidal to canalicular vesicle traffic (data not shown).

Our studies (Figs. 7-9) confirmed the observations of others that the Golgi apparatus, TGN, lysosomes, and, likely, sorting and late endosomes localize to the pericanalicular region.[33,45,46] Because hepatocytes also initiate endocytosis from the canalicular membrane,[33] this region, which contains EEA1-tagged vesicles (Fig. 8) likely also contains the hepatocyte subapical compartment.[33,47]

This spatial pattern of endosome distribution was altered by CTX, PTX, and 17-hour, but not 1-hour, exposure to dibutyryl cAMP. In CTX-treated liver, TR-dextran–containing vesicles were seen both randomly distributed in the cytoplasm and clustered in a unique perinuclear position (Fig. 10). These perinuclear endocytic vesicles may include both early and late endosomes as some vesicles colocalized with markers of both (EEA1, transferrin receptors, LAMP-1) (Figs. 8 and 9). Because vesicles were tightly packed in the perinuclear region, it was not possible to determine if all of these markers colocalized to the same vesicles. Some of these perinuclear vesicles may be lysosomes, because they persisted after an overnight chase of probe (Fig. 10J) and they were visible as perinuclear autofluorescent granules in CTX-treated livers not injected with TR-dextran (data not shown). Although TGN-38 also was mislocalized to the perinuclear area in CTX-treated livers (Fig. 7D), TR-dextran did not colocalize with TGN-38, indicating that trafficking of endocytic structures and TGN marker proteins were altered separately by CTX.

Although confocal microscopy is not quantitative, inspection of these images suggested that these perinuclear vesicles may account for much of the extra endocytosed probe found in CTX-treated livers (Fig. 2). This perinuclear location is similar to the location of recycling endosomes, late endosomes, and lysosomes in nonpolarized cultured cells. Indeed, in cultured hepatocytes, ligands and membrane proteins traffic from perisinusoidal endosomes through a juxtanuclear compartment to the canaliculus.[48] Therefore, both lengthy exposure to cAMP and cell culture may change endosome trafficking to include a juxtanuclear compartment.

Our data do not indicate whether all of these toxin/cAMP-induced changes in endosome ion transport, FPE, and vesicle trafficking were the result of changes in one specific step during endocytosis. However, proper sorting of endosome contents, recycling of receptors, and endosome maturation in liver all appear to require the correct association of endosomes with microtubules.[49-51] Thus, a partial block at the point where sorting endosomes transfer fluid-phase probes into recycling endosomes might account for our data, if such a block altered attachment of endosomes to microtubules and translocation to the canaliculus.[49-51] Alternatively, if endocytosis were blocked at the sorting stage, sorting endosomes might accumulate, saturating the translocation process. Could these changes in endocytosis be caused simply by an increased turnover rate of the vacuolar H^+-ATPase, leading to a more acid pH_i? This seems unlikely because although elimination of vesicle acidity blocks transfer of cargo from early to late endosomes and lysosomes,[6,7] the changes in pH_i were small (Table 1) and there is no evidence that a more acidic pH_i blocks endosome trafficking.

The specific signal transduction pathways responsible for these changes in liver endocytosis are not known. Although CTX and PTX each likely interact with a variety of signal transduction cascades, the common factor is an increase in cAMP,[14] because CTX directly activates G_{sa} and adenylate cyclase, while PTX inactivates G_{ia}, releasing tonic inhibition of adenylate cyclase. Furthermore, most of the effects we identified were reproduced by a short exposure to cAMP (Figs. 1 and 5), which might function, as suggested for regulation of Ntcp,[52] through protein kinase B. However, 1 hour of dibutyryl cAMP did not cause detectable accumulation of mistrafficked perinuclear vesicles, an effect that might require pro-

longed exposure to cAMP. Furthermore, only CTX appeared to density-shift endosomes at early time points (Fig. 2). This could have been a unique effect of Gsa, not mediated by cAMP, a result of the high levels of cAMP generated by CTX[14] or an effect only seen when time points shorter than 20 minutes were examined.

In summary, we have shown that CTX and other agents that increase cAMP caused substantial changes in hepatocyte endocytosis. It is unlikely that all of these effects could be explained simply by an increase in the numerical density or turnover rate of the vacuolar H^+-ATPase. More likely, these agents altered specific steps in fusion/remodeling of early to late endosomes/lysosomes, and our findings implicated changes in recycling and efflux of endocytosed probe and in trafficking of vesicles. It is not known whether all of these effects of CTX are related. If so, it would suggest that maturation and/or remodeling of endosomes: 1) involves specific membrane proteins, such as ion transporters, as well as receptors and cargo; 2) is dependent on or itself regulates microtubule-based vesicle trafficking; and 3) may, if altered, alter rates of cargo recycling.

Acknowledgment: The author thanks Dr. Dietrich Keppler for his gift of antibody to MRP-2, Chris Edwards and Bruce Donohue for assistance with confocal microscopy, and Mr. James Beals (PhotoGraphics) for imaging processing.

REFERENCES

1. Steer CJ. Receptor-mediated endocytosis: mechanism, biologic function, and molecular properties. In: Zakim D, Boyer TD, eds. Hepatology. Vol 1, 3rd ed. Philadelphia: Saunders, 1996:149-214.
2. Mukherjee S, Ghosh RN, Maxfield FR. Endocytosis. Physiol Rev 1997; 77:759-803.
3. Stoorvogel W, Strous GJ, Geuze HJ, Oorschot V, Schwartz AL. Late endosomes derive from early endosomes by maturation. Cell 1991;65:417-427.
4. Stevens TH, Forgac M. Structure, function and regulation of the vacuolar (H^+)-ATPase. Cell Dev Biol 1997;13:779-808.
5. Van Dyke RW. Na^+/H^+ exchange modulates acidification of early rat liver endocytic vesicles. Am J Physiol 1995;269:C943-C954.
6. Van Weert AWM, Dunn KW, Geuze HJ, Maxfield FR, Stoorvogel W. Transport from late endosomes to lysosomes, but not sorting of integral membrane proteins in endosomes, depends on the vacuolar proton pump. J Cell Bio 1995;130:821-834.
7. Clague MJ, UrbeS, Aniento F, Gruenberg J. Vacuolar ATPase activity is required for endosomal carrier vesicle formation. J Biol Chem 1994;269: 21-24.
8. Emans N, Verkman AS. Real-time fluorescence measurement of cell-free endosome fusion: regulation by second messengers. Biophys J 1996;71: 487-494.
9. Hansen SH, Casanova JE. Gsα stimulates transcytosis and apical secretion in MDCK cells through cAMP and protein kinase A. J Cell Biol 1994;126:677-687.
10. Helms JB. Role of heterotrimeric GTP binding proteins in vesicular protein transport: indications for both classical and alternative G protein cycles. FEBS Lett 1995;369:84-88.
11. Bradbury NA, Bridges RJ. Role of membrane trafficking in plasma membrane solute transport. Am J Physiol 1994;267:C1-C24.
12. Mukhopadhayay S, Anathanarayanan M, Stieger B, Meier PJ, Suchy FJ, Anwer MS. cAMP increases liver Na^+-taurocholate cotransport by translocating transporter to plasma membranes. Am J Physiol 1997;273: G842-G848.
13. Gatmaitan ZC, Nies AT, Arias IM. Regulation and translocation of ATP-dependent apical membrane proteins in rat liver. Am J Physiol 1997;272: G1041-G1049.
14. Van Dyke RW. Cholera and petussis toxins increase acidification of endocytic vesicles without altering ion conductances. Am J Physiol 1997; 272:C1123-C1133.
15. Van Dyke RW. Acidification of rat liver lysosomes: quantitation and comparison with endosomes. Am J Physiol 1993;265:C901-C917.
16. Van Dyke RW, Belcher JD. Acidification of three types of liver endocytic vesicles: similarities and differences. Am J Physiol 1994;266:C81-C94.
17. Van Dyke RW. Acidification of lysosomes and endosomes. In: Lloyd JB, Mason RW, eds. Subcellular Biochemistry. Vol 27. Biology of the Lysosome. New York: Plenum, 1996:331-360.
18. Van Dyke RW, Barns DW, Lewis ML. Effects of cholera toxin, cAMP, fasting and perfusion on rat liver fluid phase endocytosis [Abstract]. HEPATOLOGY 1999:30:505A.
19. Roelofsen H, Bakker CTM, Schoemaker B, Heijn M, Jansen PLM, Elferink RPJ. Redistribution of canalicular organic anion transport activity in isolated and cultured rat hepatocytes. HEPATOLOGY 1995;21:1649-1657.
20. Westwick, JK, Fleckenstein J, Yin M, Yang SQ, Bradham CA, Brenner DA, Diehl AM. Differential regulation of hepatocyte DNA synthesis by cAMP in vitro and in vivo. Am J Physiol 1996;271:G780-G790.
21. Bartles JR, Braiterman LT, Hubbard AL. Endogenous and exogenous domain markers of the rat hepatocyte plasma membrane. J Cell Biol 1985;100:1126-1138.
22. Lencer WI, Weyer P, Verkman AS, Ausiello DA, Brown D. FITC-dextran as a probe for endosome function and localization in kidney. Am J Physiol 1990;258:C309-C317.
23. Meier PJ, Sztul ES, Reuben A, Boyer JL. Structural and functional polarity of canalicular and basolateral plasma membrane vesicles isolated in high yield from rat liver. J Cell Biol 1984;98:991-1000.
24. Sheff, DR, Daro EA, Huff M, Mellman I. The receptor recycling pathway contains two distinct populations of early endosomes with different sorting functions. J Cell Biol 1999;145:123-139.
25. Harman D. Lipofuscin and ceroid formation: the cellular recycling system. In: Porta EA, ed. Lipofuscin and Ceroid Pigments. New York: Plenum, 1990:3-15.
26. Buchler M, Konig J, Brom M, Kartenbeck J, Spring H, Horie T, Keppler D. cDNA cloning of the hepatocyte canalicular isoform of the multidrug resistance protein, cMrp, reveals a novel conjugate export pump deficient in hyperbilirubinemic mutant rats. J Biol Chem 1996;271:15091-15098.
27. Christoforidis S, McBride HM, Burgoyne RD, Zerial M. The Rab5 effector EEA1 is a core component of endosome docking. Nature 1999;397:621-625.
28. Ponnambalam S, Rabouille C, Luzio JP, Nilsson T, Warren G. The TGN38 glycoprotein contains two non-overlapping signals that mediate localization to the Trans-Golgi Network. J Cell Biol 1994;125:253-268.
29. Lippincott-Schwartz J, Fambrough DM. Lysosomal membrane dynamics: structure and interorganellar movement of a major lysosomal membrane glycoprotein. J Cell Biol 1986;102:1593-1605.
30. Novick P, Zerial M. The diversity of Rab proteins in vesicle transport. Curr Opin Cell Biol 1997;9:496-504.
31. Van Dyke RW. Effect of cholera toxin on rat liver lysosome acidification. Biochem Biophys Res Commun 2000;274:717-721.
32. Pol A, Ortega D, Enrich C. Identification and distribution of proteins in isolated endosomal fractions of rat liver: involvement in endocytosis, recycling and transcytosis. Biochem J 1997;323:435-443.
33. Tuma PL, Finnegan CM, Yi JH, Hubbard AL. Evidence for apical endocytosis in polarized hepatic cells: phosphoinositide 3-kinase inhibitors lead to the lysosomal accumulation of resident apical plasma membrane proteins. J Cell Biol 1999;145:1089-1102.
34. Paloheimo M, Linkola J, Lempinen M, Folke M. Time-courses of hepatocellular hypopolarization and cyclic adenosine 3′,5′-monophosphate accumulation after partial hepatectomy in the rat. Gastroenterology 1984;87:639-646.
35. Zdankiewicz P, Nathan JD, Niazi Z, Spector SA, Wang JP, Seymour NE, Geibel JP, et al. Regulation of hepatocyte endocytosis by feeding is impaired in chronic pancreatitis (CP) [Abstract]. Gastroenterology 1997: 112:A496.
36. Roelofsen H, Soroka CJ, Keppler D, Boyer JL. Cyclic AMP stimulates sorting of the canalicular organic anion transporter (Mrp2/cMoat) to the apical domain in hepatocyte couplets. J Cell Sci 1998;111:1137-1145.
37. Hayakawa T, Bruck R, Ng OC, Boyer JL. DBcAMP stimulates vesicle transport and HRP excretion in isolated perfused rat liver. Am J Physiol 1990;259:G727-G735.
38. Van Dyke RW, Root KV, Hsi RA. cAMP and protein kinase A stimulate acidification of rat liver endosomes in the absence of chloride. Biochem Biophys Res Commun 1996;222:312-316.
39. Munniksma J, Noteborn M, Kooistra T, Stienstra S, Bouma JMW, Gruber M, Brouwer A, et al. Fluid endocytosis by rat liver and spleen. Experiments with ^{125}I-labelled poly (vinylpyrrolidone) in vivo. Biochem J 1980; 192:613-621.

40. Ose L, Ose T, Reinertsen R, Berg T. Fluid endocytosis in isolated rat parenchymal and non-parenchymal liver cells. Exp Cell Res 1980;126: 109-119.
41. Scharschmidt BF, Lake JR, Renner EL, Licko V, Van Dyke RW. Fluid phase endocytosis by cultured rat hepatocytes and perfused rat liver: implications for plasma membrane turnover and vesicular trafficking of fluid phase markers. Proc Natl Acad Sci U S A 1986;83:9488-9492.
42. Blomhoff R, Nenseter MS, Green MH, Berg T. A multicompartmental model of fluid-phase endocytosis in rabbit liver parenchymal cells. Biochem J 1989;262:605-610.
43. Nakano A, Marks DL, Tietz PS, De Groen PC, LaRusso NF. Quantitative importance of biliary excretion to the turnover of hepatic lysosomal enzymes. HEPATOLOGY 1995;22:262-266.
44. Novikoff PM, Cammer M, Tao L, Oda H, Stockert RJ, Wolkoff AW, Satir P. Three-dimensional organization of rat hepatocyte cytoskeleton: relation to the asialoglycoprotein endocytosis pathway. J Cell Sci 1996;109:21-32.
45. Ortega D, Pol A, Biermer M, Jackle S, Enrich C. Annexin VI defines an apical endocytic compartment in rat liver hepatocytes. J Cell Sci 1998; 111:261-269.
46. Poucell-Hatton S, Brant J, Haley D, Martone M, Lamont S, Ellisman M, Hardison W. Three dimensional reconstruction of the Golgi Apparatus and bile canaliculus in the whole rat hepatocyte [Abstract]. Gastroenterology 1997:112:A14.
47. Van Ijzendoorn SC, Hoekstra D. The subapical compartment: a novel sorting center? Trends Cell Biol 1999;9:144-149.
48. Hemery I, Durand-Schneider AM, Feldmann G, Vaerman JP, Maurice M. The transcytotic pathway of an apical plasma membrane protein (B10) in hepatocytes is similar to that of IgA and occurs via a tubular pericentriolar compartment. J Cell Sci 1996;109:1215-1227.
49. Murray JW, Bananis E, Wolkoff AW. Reconstitution of ATP-dependent movement of endocytic vesicles along microtubules in vitro: an oscillatory bidirectional process. Mol Biol Cell 2000;11:419-433.
50. Aniento F, Eman N, Griffiths G, Gruenberg J. Cytoplasmic dynein-dependent vesicular transport from early to late endosomes. J Cell Biol 1993;123:1373-1387.
51. Maples CJ, Ruiz WG, Apodaca G. Both microtubules and actin filaments are required for efficient postendocytotic traffic of the polymeric immunoglobulin receptor in polarized Madin-Darby canine kidney cells. J Biol Chem 1997;272:6741-6751.
52. Webster CRL, Anwer MS. Role of the PI3K/PKB signaling pathway in cAMP-mediated translocation of rat liver Ntcp. Am J Physiol 1999;277: G1165-G1172.